Journal of Molecular Catalysis A: Chemical 423 (2016) 151–159

Contents lists available at ScienceDirect

Journal of Molecular Catalysis A: Chemical

journal homepage: www.elsevier.com/locate/molcata

New insights into the effects of Mn and Li on the mechanistic pathway for CO hydrogenation on Rh-Mn-Li/SiO_2 catalysts

Jun Yu [a], Dongsen Mao [a,*], Dan Ding [a], Xiaoming Guo [a], Guanzhong Lu [a,b,*]

[a] Research Institute of Applied Catalysis, School of Chemical and Environmental Engineering, Shanghai Institute of Technology, Shanghai 201418, China
[b] Key Laboratory for Advanced Materials and Research Institute of Industrial catalysis, East China University of Science and Technology, Shanghai 200237, China

ARTICLE INFO

Article history:
Received 14 April 2016
Received in revised form 2 June 2016
Accepted 20 June 2016
Available online 21 June 2016

Keywords:
Rh-Mn-Li/SiO_2 catalysts
CO hydrogenation
C_2^+ oxygenates synthesis
Mechanistic pathway

ABSTRACT

It has been reported widely that Rh-Mn-Li/SiO_2 catalysts can exhibit high selectivity to C_2^+ oxygenates during CO hydrogenation, with promoters of Mn and Li playing an important role in this behavior. In this study, a series catalysts of Rh-Mn-Li/SiO_2 with different amounts of Mn and Li were prepared, and the new insights into the effects of Mn and Li on the mechanistic pathway for C_2^+ oxygenates synthesis from syngas were investigated. The XPS analysis showed that Rh existed mainly as metallic Rh after reduction, however partially positively charged $Rh^{\delta+}$ atoms appeared on the surface of Mn-containing catalyst due to the interaction of Rh-Mn. The results of H_2-TPR indicated that both of Li and Mn can inhibit the reduction of Rh_2O_3. With the increase in the ratio of Mn/Rh, the most effective interaction, associated to the presence of two reduction centers of Rh_2O_3, was obtained when the ratio of Mn/Rh = 1. *In situ*-FTIR was used to probe the effects of Mn and Li on CO absorption and hydrogenation. With regards to the CO adsorption, the doping of Mn can enhance the CO adsorption ability of Rh and weaken the CO-Rh bond strength very effectively when the amount of Mn reached 1.5 wt.%. Improved capacity of CO adsorption is conducive to increase of CO conversion, while the weakening of CO-Rh bond is beneficial to the CO insertion reaction, thus contributing to the generation of C_2^+ oxygenates. Moreover, the low amount of Li ($\leq$0.075 wt.%) can also enhance the CO adsorption, resulting in the improvement of reactivity. On the other hand, Mn and Li promoted dissociation of H_2, which is favorable to an increase in the rate of hydrogenation. But an opposite effect appeared at high content of Mn (>1.5 wt.%). As the optimized results, when Rh, Mn, Li content was 1.5 wt.%, 1.5 wt.% and 0.075 wt.%, the catalyst for CO hydrogenation of C_2^+ oxygenates achieved the best performance of C_2^+ oxygenates synthesis.

1. Introduction

The search for processes to provide alternative feedstock for fuels has been promoted by the increasing concerns about global climate change, depletion of fossil fuel resources, and rising crude oil prices. Ethanol has attracted increasing attention as a clean fuel or an additive to gasoline [1,2]. Direct catalytic synthesis of C_2 oxygenates (*e.g.*, ethanol, acetaldehyde and acetic acid) from syngas, which can be derived from biomass, coal, or natural gas, is one of the most promising technologies [3,4]. However, developing an efficient and selective catalyst for C_2 oxygenates synthesis has been a major challenge.

Over the last thirty years, Rh-based catalysts have been found to display unique efficiency and selectivity in C_2 oxygenates synthesis from syngas [5–9]. Since single Rh component exhibits a poor activity and mainly leads to formation of hydrocarbon products, with methanol being the primary oxygenate, efforts have been centered on improving the dispersion of Rh and modification of Rh with additives and supports in order to selectively synthesize C_2 oxygenates [10–12]. So far, the catalyst of Rh-Mn-Li/SiO_2 was found to give an excellent activity and C_2 oxygenates selectivity [13], with promoters of Mn and Li playing an important role in this behavior.

Considerable investigations heretofore have been reported to interpret the role of Mn and Li. Sachtler et al. [14] concluded that the improved activity of Mn promoted Rh/SiO_2 catalysts was due to the formation of a tilted CO adsorption mode on the Rh surface. The tilted adsorbed CO dissociated more easily, thereby increasing the CO hydrogenation activity. Wang et al. [15] proposed that the interaction between Rh and Mn formed a new active site of

* Corresponding authors at: Research Institute of Applied Catalysis, School of Chemical and Environmental Engineering, Shanghai Institute of Technology, Shanghai 201418, China
E-mail addresses: dsmao@sit.edu.cn (D. Mao), gzhlu@ecust.edu.cn (G. Lu).

http://dx.doi.org/10.1016/j.molcata.2016.06.018
1381-1169/

($Rh_x{}^0Rh_y{}^+$)-O-M^{n+}, wherein a portion of the Rh was present in the Rh^+ oxidation state, the promoter Mn (M^{n+}) was in close contact with these Rh species, and the formation of this active site was conducive to the C_2 oxygenates synthesis. With respect to Li, it is believed that addition of Li can restrain CO dissociation, thereby improving the selectivity of oxygenates [16]. Chuang et al. [17] reported that the effect of Li promoter was attributed to electron-donation, which inhibited the hydrogenation ability of the catalyst and hence promoted the formation of oxygenates. Although a lot of experiments and reasoning were focused on the interaction mechanism among Rh, Mn, and Li, the synergistic promoting roles of Mn and Li cannot be confined to one of the theories mentioned above due to the varied experimental conditions and complex reaction scheme.

In the present study, to further probe the promoting mechanisms of Mn and Li, the catalytic activities of Rh/SiO_2 catalysts promoted with various amounts of Mn and Li for CO hydrogenation were compared. Considering that the catalytic performance of the Rh-Mn-Li/SiO_2 catalyst for the synthesis of C_2 oxygenates from CO hydrogenation was enhanced greatly when a commercial SiO_2 was replaced by a monodispersed SiO_2 prepared by the Stöber method [18,19], the monodispersed SiO_2 was employed in serving as the support for Rh-based catalysts. The techniques of XPS and H_2-TPR were used to relate to the structure-activity relationships of the catalysts. Furthermore, new insights into the effects of Mn and Li on the mechanistic pathway for CO hydrogenation were demonstrated by diffuse reflectance infrared Fourier transform spectroscopy (DRIFTS).

2. Experimental

2.1. Catalyst preparation

SiO_2 was prepared by the Stöber method [20] as follows. The mixture solution of 21 mL tetraethylorthosilicate (TEOS) (99.5%, SCRC) and 50 mL anhydrous ethanol (99.7%, SCRC) was added slowly into the solution of 76 mL $NH_3{\cdot}H_2O$ (26 vol%, SCRC) and 200 mL anhydrous ethanol. Then, this synthesized solution was aged for 4 h and separated centrifugally at 7000 rpm. Finally, the collected product was washed with de-ionized water three times and dried at 70 °C for 12 h. Before used, it was calcined in static air at 350 °C for 4 h.

$RhCl_3$ hydrate (Rh ~36 wt.%, Fluka), $Mn(NO_3)_2{\cdot}6H_2O$ (99.99%, SCRC), Li_2CO_3 (99.5%, SCRC), and SiO_2 mentioned above were used in catalyst preparations. Catalysts were prepared by co-impregnation to incipient wetness of silica (1.0 g) with an aqueous solution of $RhCl_3$ hydrate and aqueous solutions of precursors of the promoters, followed by drying at 90 °C for 4 h, and then at 120 °C overnight before being calcined in air at 350 °C for 4 h. The specific content of various metals are listed in related tables and figures. For example, the catalyst referred to as 1.5Rh-1.5Mn-0.075Li/SiO_2 indicated that the weight percents of Rh, Mn and Li were 1.5 wt.%, 1.5 wt.%, and 0.075 wt.%, respectively. Elemental analysis by inductively coupled plasma (ICP) revealed good agreement between the expected and experimental values. In addition, the possible chloride composition in the catalyst after calcination was also detected by ICP, and the absence of chloride was confirmed.

2.2. Reaction

CO hydrogenation was performed in a fixed-bed micro-reactor with length ~350 mm and internal diameter ~5 mm. The catalyst (0.3 g) diluted with inert α-alumina (1.2 g) was loaded between quartz wool and axially centered in the reactor tube, with the temperature monitored by a thermocouple close to the catalyst bed. Prior to reaction, the catalyst was heated to 400 °C (heating rate ~3 °C/min) and reduced with 10% H_2/N_2 (total flow rate = 50 mL/min) for 2 h at atmospheric pressure. The catalyst was then cooled down to 300 °C and the reaction started as gas flow was switched to a H_2/CO mixture (molar ratio of H_2/CO = 2, total flow rate = 50 mL/min) at 3 MPa. All post-reactor lines and valves were heated to 150 °C to prevent product condensation. The products were analyzed on-line (Agilent GC 6820) using a HP-PLOT/Q column (30 m, 0.32 mm ID) with detection with an FID (flame ionization detector) and a TDX-01 column with a TCD (thermal conductivity detector). The conversion of CO was calculated based on the fraction of CO that formed carbon-containing products according to: $\%Conversion = (\sum n_i M_i / M_{CO}) \cdot 100$, where n_i is the number of carbon atom in product i, M_i is the percentage of product i detected, and M_{CO} is the percentage of carbon monoxide in the syngas feed. The selectivity of a certain product was calculated based on carbon efficiency using the formula $n_i C_i / \sum n_i C_i$, where n_i and C_i are the carbon atom number and molar concentration of the *i*th product, respectively.

2.3. Catalyst characterization

The X-ray powder diffraction (XRD) spectra of samples were obtained on a Rigaku D/MAX-IIIA X-ray diffractometer with CuKα ($\lambda = 0.15418$ nm). The specific surface area (S_{BET}), pore volume (V_p), and pore diameter (D_p) of sample were obtained by N_2 adsorption at −196 °C on a Micromeritics ASAP 2020 apparatus. The metal loadings of the catalysts were determined by ICP-OES (PerkinElmer Optima 7000DV).

The amount of hydrogen adsorption of various catalysts was calculated on the basis of H_2-TPD profiles. For H_2-TPD measurements, the catalyst (0.1 g) was reduced in-situ for 2 h at 400 °C in 10% H_2/N_2, and then was held at 400 °C for another 30 min before being cooled down to room temperature in He flow. The next step was H_2 adsorption at room temperature for 0.5 h, and then the gas was swept again with He for 3 h. Subsequently, the sample was heated in a flowing He stream (50 mL/min) up to ~500 °C at a rate of 10 °C/min, while the desorbed species was detected with a TCD detector. The uptake of H_2 was used to calculate Rh metal dispersion and particle size, assuming that each surface metal atom adsorbs one H atom, *i.e.* $H/Rh_{surface} = 1$.

Photoelectron spectra (XPS) were acquired with an ESCALAB 250Xi spectrometer in the pulse-count mode at a pass energy of 20 eV using an Al Kα ($h\nu = 1486.6$ eV) X-ray source. Kinetic energies of photoelectrons were measured using a hemispherical electron analyzer working in the constant pass energy mode. The background pressure in the analysis chamber was kept below 7×10^{-9} mbar during data acquisition. The powder samples were pressed into copper holders and then mounted on a support rod placed in the pretreatment chamber. Samples were reduced in situ at 400 °C for 1 h under 200 mbar H_2 pressure. The binding energies were calibrated relative to the C 1s peak from carbon contamination of the samples at 284.9 eV to correct for contact potential differences between the sample and the spectrometer. The XPS data were signal averaged for 20 scans and were taken in increments of 0.1 eV with dwell times of 50 ms.

H_2 temperature-programmed reduction (TPR) was carried out in a quartz microreactor. 0.1 g of the as-prepared sample was first pretreated at 350 °C in O_2/N_2 (molar ratio of $O_2/N_2 = 1/4$) for 1 h prior to a TPR measurement. During the TPR experiment, H_2/N_2 (molar ratio of $H_2/N_2 = 1/9$) was used at 50 mL/min and the temperature was ramped from room temperature to 500 °C at 10 °C/min while the effluent gas was analyzed with a TCD.

CO adsorption was studied using a Nicolet 6700 FT-IR spectrometer equipped with a Harrick diffuse reflectance infrared Fourier transform (DRIFT) cell with CaF_2 windows. Prior to exposure to the

Table 1
Catalytic activities of non-promoted and promoted Rh/SiO_2 catalysts[a].

Catalyst[b]	CO conv. (C%)	TOF[c] (s^{-1})	Selectivity of products (C%)							STY(C_2^+ Oxy) (g/(kg h))
			CO_2	CH_4	MeOH	AcH	EtOH	C_2^+ Oxy[d]	C_2^+ HC[e]	
$1.5Rh/SiO_2$	5.7	0.075	21.2	15.2	15.1	5.2	8.1	13.3	35.3	24.4
$1.5Rh\text{-}0.075Li/SiO_2$	6.1	0.076	19.1	11.5	10.4	8.3	8.8	19.4	39.6	38.9
$1.5Rh\text{-}1.5Mn/SiO_2$	11.5	0.125	14.7	14.4	8.2	10.8	12.4	24.4	38.3	91.6
$1.5Rh\text{-}1.5Mn\text{-}0.075Li/SiO_2$	18.9	0.194	1.1	12.1	2.3	25.4	27.1	54.3	30.2	309.1

[a] Reaction conditions: P = 3 MPa, Catalyst: 0.3 g, and flow rate = 50 mL/min (H_2/CO = 2), data taken after 15 h when steady state reached. Experimental error: ±5%.
[b] The numbers in the parenthesis indicate the weight percentage relative to the initial weight of the support material.
[c] TOF based on CO conversion and H_2 chemisorption.
[d] C_2^+ Oxy denotes oxygenates containing two and more carbon atoms.
[e] C_2^+ HC denotes hydrocarbons containing two and more carbon atoms.

Table 2
Effect of Mn loading on CO hydrogenation over $Rh\text{-}Mn\text{-}Li/SiO_2$ catalyst[a].

Rh/Mn[b]	CO conv. (C%)	TOF (s^{-1})	Selectivity of products (C%)							*STY* (C_2^+ Oxy) (g/(kg h))
			CO_2	CH_4	MeOH	AcH	EtOH	C_2^+ Oxy	C_2^+ HC	
1.5:0.5	12.0	0.142	3.6	8.8	2.6	36.8	17.8	58.5	35.5	203.4
1.5:1.0	12.8	0.139	3.6	10.1	3.2	30.0	23.2	56.4	37.0	215.1
1.5:1.5	18.9	0.194	1.1	12.1	2.3	25.4	27.1	54.3	30.2	309.1
1.5:2.5	10.1	0.126	10.1	12.1	2.3	25.0	15.6	43.5	44.2	123.1

[a] Reaction conditions as above. Experimental error: ±5%.
[b] Weight ratio of Rh/Mn, while the weight ratio of Rh/Li in all the samples = 1.5:0.075.

Table 3
Effect of Li loading on CO hydrogenation over $Rh\text{-}Mn\text{-}Li/SiO_2$ catalyst[a].

Rh/Li[b]	CO conv. (C%)	TOF (s^{-1})	Selectivity of products (C%)							*STY* (C_2^+ Oxy) (g/(kg h))
			CO_2	CH_4	MeOH	AcH	EtOH	C_2^+ Oxy	C_2^+ HC	
0	11.5	0.125	14.7	14.4	8.2	10.8	12.4	24.4	38.3	91.6
1.5:0.05	12.9	0.132	6.4	12.6	2.5	20.8	23.6	47.1	31.4	180.7
1.5:0.075	18.9	0.194	1.1	12.1	2.3	25.4	27.1	54.3	30.2	309.1
1.5:0.15	12.5	0.132	8.1	12.3	2.1	24.1	18.7	43.2	34.3	158.6
1.5:0.45	8.2	0.087	8.9	12.5	2.5	23.7	16.2	41.9	34.2	102.6

[a] Reaction conditions as above. Experimental error: ±5%.
[b] Weight ratio of Rh/Li, while the weight ratio of Rh/Mn in all the samples = 1.5:1.5.

reaction gas, the sample in the cell was pretreated in 10% H_2/N_2 (50 mL/min) at 400 °C for 2 h, followed by N_2 (50 mL/min) flushing at this temperature for 30 min. During cooling down to the room temperature in N_2, a series of background spectra were taken at different temperatures. Then, 1% CO/N_2 (50 mL/min) was introduced into the cell and the IR spectra at the desired temperatures were recorded. After heating up to 300 °C in CO/N_2 mixture for 60 min, a H_2 flow (1 mL/min) was added into the flowing CO/N_2, and the IR spectra were recorded as a function of time. Ultrahigh-purity N_2, H_2 and CO used in the IR investigations were further purified by dehydration and deoxygenization. The spectral resolution was 4 cm^{-1} with 64 interferograms being added to obtain a satisfactory signal-to-noise ratio.

3. Results and discussions

3.1. Catalytic performances

Table 1 compares the catalytic activities of the non-promoted and Mn and/or Li promoted Rh/SiO_2 catalysts for CO hydrogenation at 300 °C. It can be seen that the $1.5Rh/SiO_2$ catalyst showed a poor catalytic performance for C_2^+ oxygenate synthesis from syngas. Addition of Mn and Li promoters modified both CO conversion and product selectivities. As listed in Table 1, adding 0.075 wt.% Li to the $1.5Rh/SiO_2$ catalyst, namely $1.5Rh\text{-}0.075Li/SiO_2$, restrained the formation of CH_4 and increased the selectivities of C_2^+ oxygenates and hydrocarbons, which indicated that Li addition promoted chain growth probability. Compared to the non-promoted catalyst, the Mn promoted Rh/SiO_2 catalyst ($1.5Rh\text{-}1.5Mn/SiO_2$) showed significant suppression of the formation of CO_2 and methanol, but the selectivities towards ethanol and acetaldehyde were higher than that of $1.5Rh/SiO_2$ catalyst. Compared to Rh/SiO_2 promoted singly by Li or Mn, the doubly promoted catalyst $1.5Rh\text{-}1.5Mn\text{-}0.075Li/SiO_2$ combined the positive promoting effects of both Li and Mn, resulting in the highest CO conversion and C_2^+ oxygenates selectivity, along with lower selectivities for CO_2, CH_4 and methanol. Moreover, the trend in turnover frequency (TOF) values of CO conversion over the catalysts was consistent with that of CO conversion.

The effect of different amounts of manganese promoter on the catalytic performance of $Rh\text{-}Mn\text{-}Li/SiO_2$ catalysts is shown in Table 2. As observed, with the increase of Mn loading, the selectivity to methanol did not change obviously, while the selectivity of methane increased. Interestingly, although the selectivity of acetaldehyde decreased with the increase of Mn loading, the CO conversion and selectivity to ethanol showed a maximum value at about Rh/Mn ratios of 1.0. It is clear that there exists an optimum Mn loading at which oxygenate formation will be maximum.

Results of CO hydrogenation over $Rh\text{-}Mn\text{-}Li/SiO_2$ catalysts with various loadings of Li are shown in Table 3. As observed, the CO conversion and selectivity of C_2^+ oxygenates increased first with the Li loading. When 0.075 wt.% Li was added into the $1.5Rh\text{-}1.5Mn/SiO_2$ catalyst, the selectivity to CO_2 decreased largely from 14.7 to 1.1%, while the CO conversion and selectivity towards C_2^+ oxygenates increased from 11.5 and 24.4% to 18.9 and 54.3%, respectively. However, the CO conversion and selectivity towards

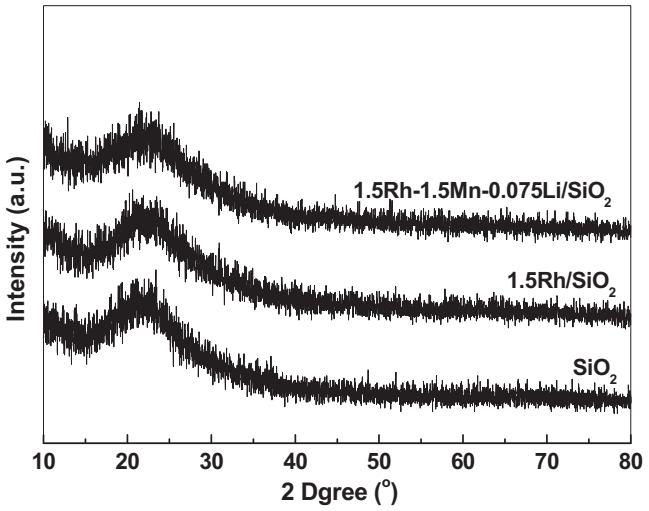

Fig. 1. The XRD patterns of support and the representative catalysts.

C_2^+ oxygenates decreased rapidly when the amount of Li exceeded 0.075 wt.%.

3.2. Textural characterization

XRD patterns of support and the representative catalysts showed no crystalline phases (Fig. 1), indicating that the SiO_2 is XRD-amorphous and the metal particles are highly dispersed on the SiO_2 support due to the small content.

N_2 adsorption-desorption was carried out to characterize the textural properties of support and the corresponding supported catalysts. As shown in Table 4, the BET surface area of SiO_2 was measured to be 11.0 m^2/g, and the BET surface areas of all the Rh-based catalysts were measured to be ca. 10.0 m^2/g. For the pore distribution, SiO_2 and the corresponding catalysts had a similar pore in the range of 7.5–8.5 nm. No significant difference was observed in the surface areas and pore sizes probably due to the fact that the concentrations of Rh and promoters were relatively low in all the catalysts prepared. Moreover, the amount of hydrogen adsorption of various catalysts calculated on the basis of their H_2-TPD profiles is summarized in Table 4, and the corresponding Rh dispersion and particle size are also exhibited. It can be seen that the doping of Mn and Li slightly improved the Rh dispersion, and, correspondingly, the Rh particle size decreased.

3.3. XPS

XPS studies have been performed to gain information about the chemical states of Rh and Mn on catalyst surfaces after reduction at 400 °C, and the results are presented in Fig. 2. It is observed that Rh existed as Rh_2O_3 (typical XPS Rh $3d_{5/2}$ at 309.2 eV, not shown) in all the fresh samples, and it is severely reduced after *in situ* pre-treatment (~307.2 eV), evidencing the presence of metallic rhodium (Rh^0). The binding energy of Rh $3d_{5/2}$ did not change as the Li promoter was added. However, after the introduction of an appropriate amount of Mn (<1.5 wt.%), the binding energy of Rh $3d_{5/2}$ shifted towards higher values (307.4–307.7 eV), indicating that the electronic density on Rh particles decreased [21]. This suggested that some partially positively charged $Rh^{\delta+}$ species also co-exist with Rh^0 on the surfaces of the reduced catalysts containing Mn promoter. Probably the presence of such oxidized Rh species might be indicative of a strong interaction of some Rh oxide particles with the assistant of Mn, considering that the electrons of rhodium atoms can be attracted by the electron-withdrawing property of Mn. Obviously, this Rh-Mn interaction would be weakened when the ratio of Mn/Rh exceeded 1.0, corresponding to that the photoelectrons binding energy of Rh $3d_{5/2}$ over 1.5Rh-2.5Mn-0.075Li/SiO_2 catalyst shifted back to ~307.3 eV. On the other hand, it can be found that the binding energy of the Mn $2p_{3/2}$ peaks were centered at about 642 eV on various Mn-containing catalysts after reduction. The XPS spectra around the Mn $2p_{3/2}$ peak between 645 eV and 641 eV cannot be deconvoluted into various Mn components of the signal (from NIST: MnO = 640.3 to 642.5 eV, MnO_2 = 641.1 to 643.4 eV, Mn_2O_3 = 641.2 to 642.8 eV, Mn_3O_4 = 641.1 to 641.9 eV) with the current spectra. Thus, it is suggested that Mn existed in the form of Mn^{2+} or higher valence states (Mn^{3+} and Mn^{4+}).

3.4. H_2-TPR

Fig. 3 shows the TPR profiles of various catalysts. It can be seen that there was only one peak at 115 °C in the TPR profile of 1.5Rh/SiO_2 catalyst, which corresponded to the reduction of Rh_2O_3 particles [22]. The reduction peak of Rh_2O_3 moved to a higher temperature (145 °C) and peak area increased pronouncedly with the addition of 0.075 wt.% Li to 1.5Rh/SiO_2 catalyst. The addition of Mn species into 1.5Rh/SiO_2 led to a split of the reduction peak of Rh_2O_3, while the reduction peak of manganese species appeared at a higher temperature (~260 °C). According to Ding's assignment, the split peaks at 105 °C and 135 °C can be ascribed to the reduction of Rh_2O_3 not intimately contacting with Mn species (denoted as Rh(I)) and of Rh_2O_3 intimately contacting with Mn species (denoted as Rh(II)), respectively [22,23]. The TPR profile of 1.5Rh-1.5Mn-0.075Li/SiO_2

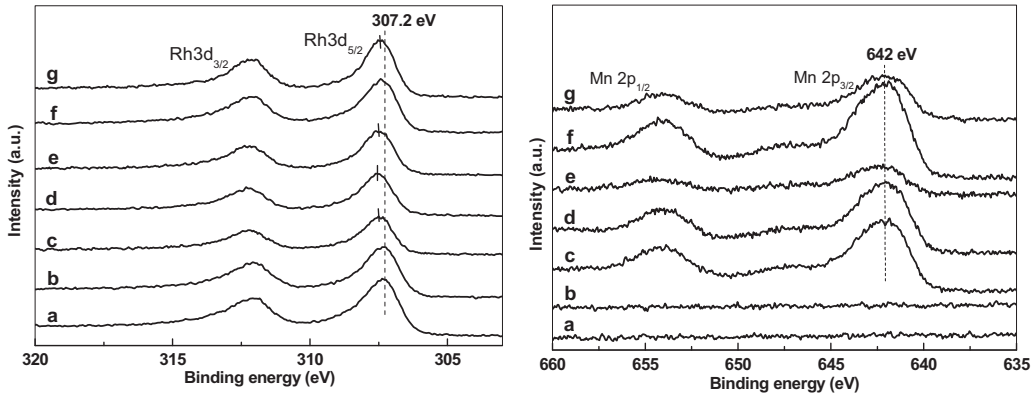

Fig. 2. XPS spectra of samples: (a) 1.5Rh/SiO_2; (b) 1.5Rh-0.075Li/SiO_2; (c) 1.5Rh-1.5Mn/SiO_2; (d) 1.5Rh-1.5Mn-0.075Li/SiO_2; (e) 1.5Rh-0.5Mn-0.075Li/SiO_2; (f) 1.5Rh-2.5Mn-0.075Li/SiO_2; (g) 1.5Rh-1.5Mn-0.45Li/SiO_2.

Table 4
Specific surface areas (S_{BET}), pore volume (V_p) and pore diameter (D_p) from N_2 adsorption-desorption and H_2 chemisorption.

Samples	S_{BET} (m^2/g)	V_p (cm^3/g)	D_p (nm)	H_2 chemisorption		
				H_{2ads} (μmol/g)	Dispersion[a] (%)	Particle size (nm)
SiO_2	11.0	0.027	8.3	–	–	–
1.5Rh/SiO_2	10.6	0.027	8.1	20	27	4.1
1.5Rh-0.075Li/SiO_2	10.4	0.026	8.0	21	29	3.9
1.5Rh-1.5Mn/SiO_2	10.1	0.025	7.7	24	33	3.4
1.5Rh-1.5Mn-0.075Li/SiO_2	10.1	0.025	7.8	26	35	3.2
1.5Rh-0.5Mn-0.075Li/SiO_2	10.3	0.026	7.9	22	30	3.7
1.5Rh-1.0Mn-0.075Li/SiO_2	10.2	0.026	7.7	24	33	3.4
1.5Rh-2.5Mn-0.075Li/SiO_2	10.0	0.024	7.6	21	29	3.9
1.5Rh-1.5Mn-0.05Li/SiO_2	10.2	0.025	7.8	26	35	3.2
1.5Rh-1.5Mn-0.15Li/SiO_2	10.2	0.026	7.7	25	34	3.3
1.5Rh-1.5Mn-0.45Li/SiO_2	10.3	0.025	7.7	25	34	3.3

[a] Assuming $H/Rh_{surface} = 1$; experimental error: ±5%.

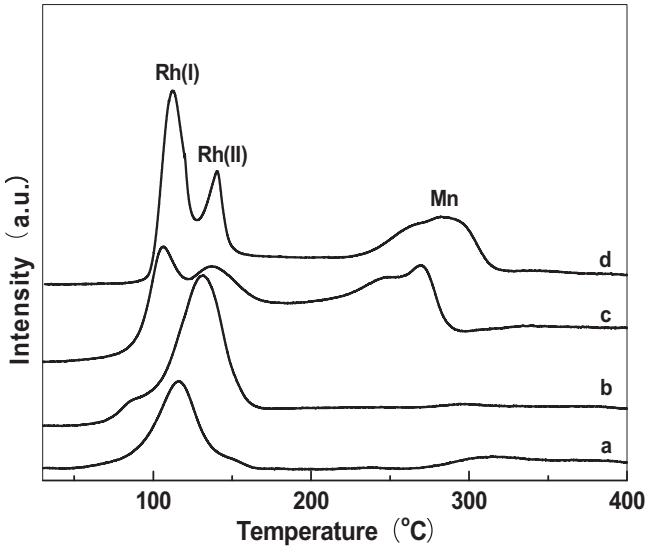

Fig. 3. The H_2-TPR profiles of the different catalysts: (a) 1.5Rh/SiO_2; (b) 1.5Rh-0.075Li/SiO_2; (c) 1.5Rh-1.5Mn/SiO_2; (d) 1.5Rh-1.5Mn-0.075Li/SiO_2.

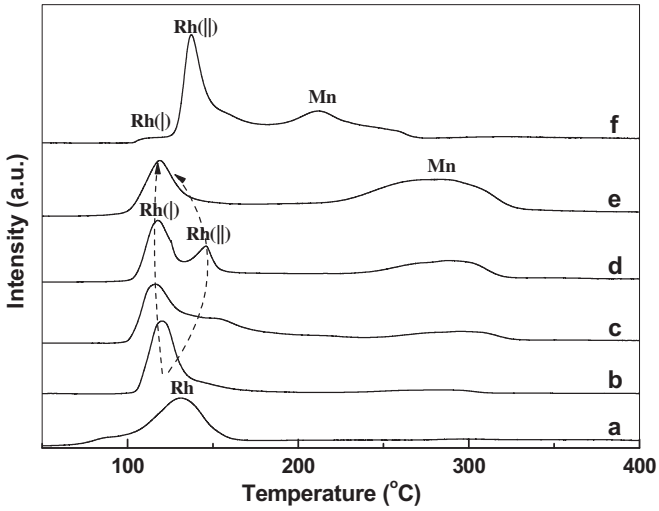

Fig. 4. The H_2-TPR profiles of the Rh-Mn-Li/SiO_2 catalysts with different Mn and Li amount: (a) 1.5Rh-0.075Li/SiO_2; (b) 1.5Rh-0.5Mn-0.075Li/SiO_2; (c) 1.5Rh-1Mn-0.075Li/SiO_2; (d) 1.5Rh-1.5Mn-0.075Li/SiO_2; (e) 1.5Rh-2.5Mn-0.075Li/SiO_2; (f) 1.5Rh-1.5Mn-0.45Li/SiO_2.

reflected the combined effect of Mn and Li. The TPR profile shape looked identical to that of 1.5Rh-1.5Mn/SiO_2, but the reduction peaks shifted to high temperature and the peaks area increased.

These results indicated that the addition of Li can inhibit the reduction of Rh_2O_3, which, in turn, was reflected by the higher reduction temperature of Rh_2O_3 caused by the presence of Li. With respect to the doping of Mn, the reduction peak of Rh_2O_3 would split into two peaks because of the interaction between Rh and Mn, suggesting that two reduction centers of Rh_2O_3 would appear by the synergism of Mn and Rh. According to the change of total area of the profiles, it is obvious that the addition of Mn and Li can increase the hydrogen consumption of Rh-based/SiO_2, which suggested that the doping of Mn and Li improves the dispersion of Rh, resulting in the increase of active centers. Some authors are of the other opinion [24] that Li can promote the overflow of surface hydrogen during the reduction process, that is to say, the dissociative hydrogen atoms can be easy to overflow into the support surface from Rh particles by assist of Li, which increases the H_2 consumption.

The TPR profiles of Rh-Mn-Li/SiO_2 catalysts with different Mn and Li loadings are shown in Fig. 4. As the amount of Mn increased from 0.5 to 1.5 wt.%, the original single reduction peak of Rh split into two reduction peaks progressively, which have been assigned to Rh(I) and Rh(II). However, when the loading of Mn reached 2.5 wt.%, the reduction of Rh_2O_3 returned to a single peak. Moreover, when the Li content was too high (0.45 wt.%), namely in the 1.5Rh-1.5Mn-0.45Li/SiO_2 catalyst, the Rh-Mn interaction was excessively enhanced, resulting in a clear increase in the peak area ratio of Rh(II) versus Rh(I) and the movement of the reduction peak of Mn to lower temperature (215 °C) compared to the 1.5Rh-1.5Mn-0.075Li/SiO_2 catalyst.

These results suggested that the intensity of Rh-Mn interaction is related to the Mn/Rh ratios. Increasing the ratio of Mn/Rh, the Rh-Mn interaction increased firstly, resulting in the presence of two reduction centers of Rh_2O_3. However, the Rh-Mn interaction decreased again when the ratio of Mn/Rh exceeded 1.0, which can be interpreted by the return of single reduction peak of Rh_2O_3 in the TPR profile of 1.5Rh-2.5Mn-0.075Li/SiO_2 catalyst. This observation is also consistent with the result of XPS. On the other hand, it is conceivable that the excess amount of Li (0.45 wt.%) would enhance the Rh-Mn interaction intensively. By combining the activities of catalysts with TPR, it is proposed that the presence of two reduction centers of Rh_2O_3 assisted by the doping of Mn is beneficial for high CO conversion and ethanol selectivity, but the excessive synergism of Mn and Rh promoted by excess doping of Li would lead to the decrease of activity.

3.5. DRIFTS study

Infrared spectroscopy provides an alternative and powerful tool to study the interaction of CO with catalysts. Firstly, Fig. 5(a) shows a series of infrared spectra acquired for the *in situ* reduced

Table 5
The frequency and peak area of the adsorbed CO species over different catalysts in Fig. 5(a).

Catalysts	Frequencies (cm^{-1})			Areas		
	CO(l)	CO(gdc)	CO(b)	CO(l)	CO(gdc)	CO(b)
1.5Rh/SiO_2	2067	–	–	0.20	–	–
1.5Rh-0.075Li/SiO_2	2067	–	–	0.18	–	–
1.5Rh-1.5Mn/SiO_2	2070	2104,2030	–	0.22	0.05	–
1.5Rh-1.5Mn-0.075Li/SiO_2	2070	2105,2032	1850	0.24	0.21	0.23
1.5Rh-2.5Mn-0.075Li/SiO_2	2067	2104,2030	1815	0.21	0.03	0.15
1.5Rh-1.5Mn-0.45Li/SiO_2	2069	2104,2030	1850	0.21	0.20	0.18

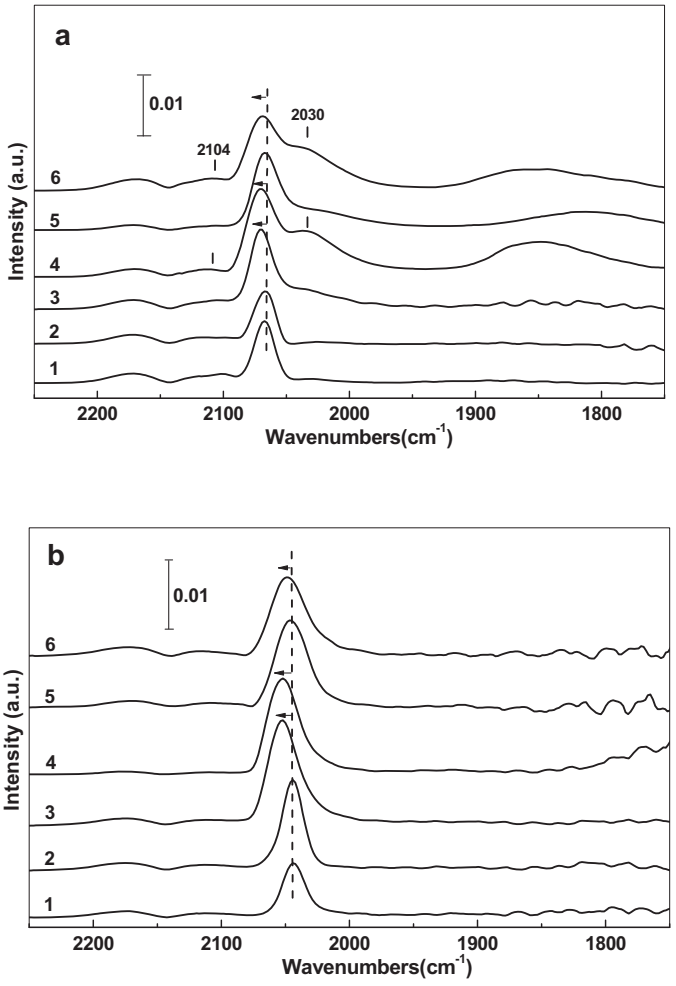

Fig. 5. The infrared spectra of chemisorbed CO at 30 °C (a) or 300 °C (b) on (1) 1.5Rh/SiO_2; (2) 1.5Rh-0.075Li/SiO_2; (3) 1.5Rh-1.5Mn/SiO_2; (4) 1.5Rh-1.5Mn-0.075Li/SiO_2; (5) 1.5Rh-2.5Mn-0.075Li/SiO_2; (6) 1.5Rh-1.5Mn-0.45Li/SiO_2 after exposing the *in situ* reduced catalysts to CO/N_2 flow for 30 min.

catalysts in the CO/N_2 flow at 30 °C. Adsorption of CO on catalyst of 1.5Rh/SiO_2 occurred mainly in two distinct modes, phase CO with characteristic bands at ca. 2180 and 2125 cm^{-1}, linear adsorbed CO [CO(l)] with adsorption band at ca. 2067 cm^{-1} [25]. It is indicated that the catalyst surface are mainly dominated by Rh^0 sites due to the general recognition that CO(l) species is formed on it [26,27]. The IR spectrum of CO adsorbed on the 1.5Rh-0.075Li/SiO_2 catalyst looked identical to that of CO adsorbed on the 1.5Rh/SiO_2 catalyst. Compared to the catalysts of 1.5Rh/SiO_2 and 1.5Rh-0.075Li/SiO_2, the position of CO(l) adsorbed on 1.5R-1.5Mn/SiO_2 catalyst shifted slightly to higher frequency, and a doublet at ~2104 and ~2030 cm^{-1} can be noticed, which is assigned to the symmetric and asymmetric carbonyl stretching of the *gem*-dicarbonyl $Rh^+(CO)_2$ [CO(gdc)] [25]. It is widely accepted that the CO(gdc) can be formed on the Rh^+ sites which may be highly dispersed [27]. This result suggested that two adsorbed sites (Rh^0 and Rh^+) appeared by the assisting of Mn, which is consistent with the result of H_2-TPR. On the other hand, the higher carbonyl stretching frequency of CO(l) may suggest less back-donation from Rh^0 into acceptor π^*_{CO} orbital, which infers that the Rh^0 sites are more electropositive caused by the electron-withdrawing effect of Mn. The XPS data characterizing the Mn promoted SiO_2-supported Rh catalysts also showed the presence of such oxidized Rh species, consistent with the above inference. Meanwhile, it also can be seen (Table 5) that the adsorption intensity of CO(l) was enhanced, suggesting that the addition of Mn could improve the dispersion of Rh. Doping of Mn and Li simultaneously (1.5Rh-1.5Mn-0.075Li/SiO_2), the intensity of CO(l) and CO(gdc) further increased, and a band at ~1830 cm^{-1} appeared, which can be attributed to bridge bonded CO [CO(b)] [9,28]. However, when the loading of Mn reached 2.5 wt.%, the position of CO(l) turned back to lower frequency and the intensity of CO(gdc) decreased clearly, proposing that Rh-Mn interaction decreased by the excessive loading of Mn, which is in good agreement with the result that the reduction of Rh_2O_3 returned single peak in the TPR profile of 1.5Rh-2.5Mn-0.075Li/SiO_2 catalyst. Moreover, the intensity of CO adsorbed on the 1.5Rh-1.5Mn-0.45Li/SiO_2 catalyst also decreased compared with that of 1.5Rh-1.5Mn-0.075Li/SiO_2 catalyst.

Fig. 5(b) shows the IR spectra of adsorbed species on the *in situ* reduced catalysts in CO/N_2 flow at 300 °C. It can be seen that all the samples only appeared the peaks of gaseous CO and CO(l), which indicated that the CO(l) species is the mainly reactive species at the reaction temperature. Compared with the catalysts of 1.5Rh/SiO_2 and 1.5Rh-0.075Li/SiO_2, the CO(l) band on the catalysts of 1.5Rh-1.5Mn/SiO_2, 1.5Rh-1.5Mn-0.075Li/SiO_2, and 1.5Rh-1.5Mn-0.45Li/SiO_2 was blue shifted. However, when the amount of Mn reached 2.5 wt.%, the CO(l) band was red shifted again.

It is obvious that the effect of Mn and Li on the state of Rh particles at the reaction temperature is similar to the situation at 30 °C. Combined with the result of H_2-TPR, it is suggested that the interaction between Rh and Mn changed by the ratio of Rh and Mn. When the ratio of Mn/Rh reached 1.0, the CO(l) band was shifted to a higher frequency, owing to the decrease of electron donation of Rh particles into the π^*_{co} orbital caused by the electron-withdrawing effect of Mn. That is to say, the shifted position of adsorbed CO also can be suggested that the CO-Rh bond strength was weakened by the assisting of Mn. Since the C_2^+ oxygenates should be formed by the reaction route-insertion of CO into a metal-CH_X bond [29,30], it is likely that the weakened CO-Rh bond is favorable for increased CO insertion, and accordingly the increase of C_2^+ oxygenates selectivity, which is good consistent with the catalytic performance. In contrast, the interaction between Rh and Mn became weakly if the content of Mn exceeded a certain value, then the CO(l) band was shifted to a lower frequency again. Correspondingly, the C_2^+ oxygenates selectivity of 1.5Rh-2.5Mn-0.075Li/SiO_2 decreased than that of 1.5Rh-1.5Mn-0.075Li/SiO_2. Moreover, the

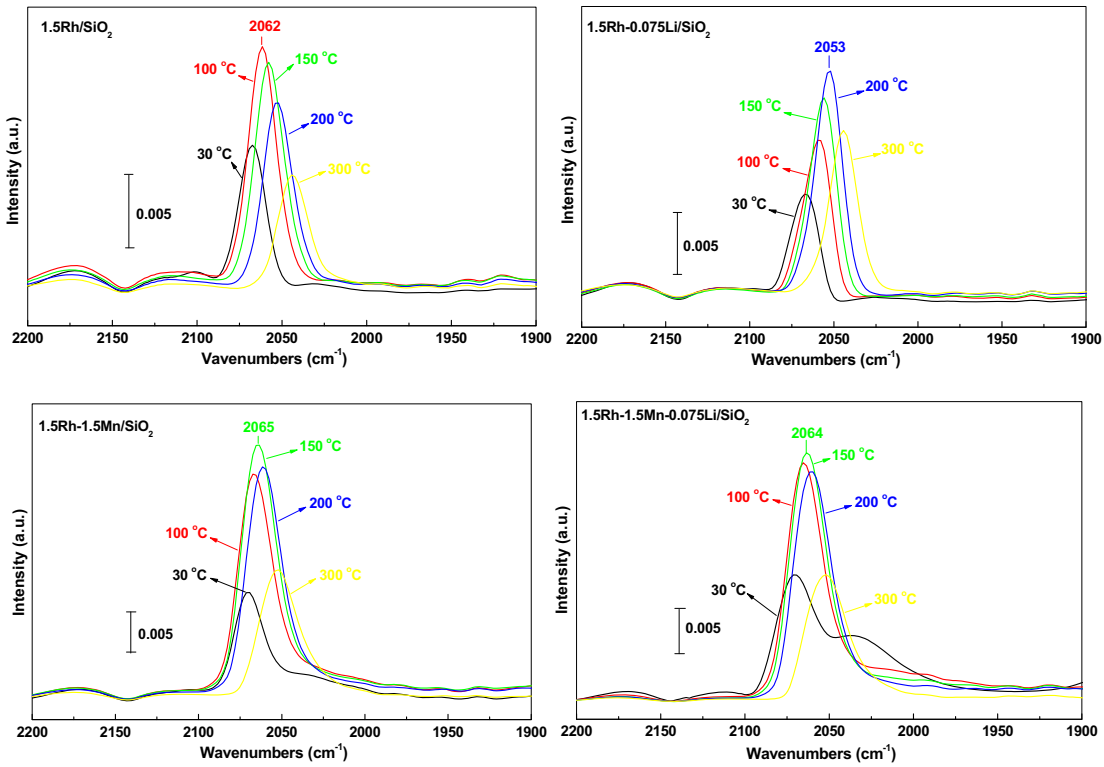

Fig. 6. The infrared spectra of adsorbed CO as a function of temperature after exposing the *in situ* reduced catalysts to CO/N_2 flow.

excessive doping of Mn and Li can weaken the adsorption ability of Rh, resulting in the decrease of CO conversion.

A series of infrared spectra of adsorbed CO over the *in situ* reduced catalysts in the CO/N_2 flow as a function of temperature are given in Fig. 6. It can be seen that the catalyst surface has been in the transformation process of adsorption and desorption. For the catalyst of $1.5Rh/SiO_2$, the amount of adsorbed CO increased as the increase of temperature, then reached a maximum at 100 °C, and decreased by the acceleration of desorption rate when the temperature further increased. Compared with the non-promoted catalyst, the desorption rate of adsorbed CO decreased by the doping of 0.075 wt.% Li, the maximum amount of adsorbed CO was reached until 200 °C. For the 1.5 wt.% Mn-containing catalyst, the desorption rate of adsorbed CO also reduced than that of $1.5Rh/SiO_2$ catalyst, the maximum peak of adsorbed CO appeared at 150 °C.

It can be inferred that the addition of 0.075 wt.% Li and/or 1.5 wt.% Mn restrains the desorption of chemisorbed CO or enhances the adsorption ability of Rh sites at the higher temperature, resulting in the more chemisorbed CO can join in the reaction under the reaction temperature. Moreover, according to the intensity of CO(l), compared with the effect of Li, the doping of Mn can enhance the ability of CO adsorption more obviously, considering that the addition of Mn could further improve the dispersion of Rh. As a result, the synergistic promoting effect of Mn and Li can be revealed on the CO conversion of catalysts as seen in Table 1.

Fig. 7 shows the IR spectra taken after CO reaction with H_2 at 300 °C on the different catalysts. For all the catalysts, the spectra looked quite similar to the spectra for CO absorbed in the absence of H_2 on the catalytic surfaces, but the intensities and wavenumbers of CO(l) decreased with different degrees as a function of time, ascribable to a decrease in dipole coupling with desorption and the decrease in surface coverage [31]. It can be seen that the rates of decrease in the band for CO(l) on different catalysts followed the order as shown in Fig. 7: $1.5Rh/SiO_2 < 1.5Rh\text{-}0.075Li/SiO_2 < 1.5Rh\text{-}2.5Mn\text{-}0.075Li/SiO_2 < 1.5Rh\text{-}1.5Mn/SiO_2 < 1.5Rh\text{-}1.5Mn\text{-}0.45Li/SiO_2 < 1.5Rh\text{-}1.5Mn\text{-}0.075Li/SiO_2$.

It is conceivable that, without the promoting effect of promoters, the dissociation ability of H_2 on Rh particles is very weak, resulting in a low hydrogenation activity. The addition of Li and/or Mn was in contact with the Rh particles, which promoted the dissociation of hydrogen, then increased the consuming of absorbed CO by hydrogenation. Compared with the $1.5Rh\text{-}1.5Mn\text{-}0.075Li/SiO_2$ catalyst, the decreasing rates of CO(l) on the catalysts of $1.5Rh\text{-}2.5Mn\text{-}0.075Li/SiO_2$ were slower. It is suggested that the higher doping amount of Mn destroyed the fitting Rh-promoter interaction, further restrained the hydrogen dissociation, which is in line with the result of H_2-TPR. In addition, the higher amount of Li (0.45 wt.%) in the catalyst can still keep a high rate of hydrogenation.

Based on the IR study, it is concluded that the addition of Mn and Li have a compositive influence on the CO adsorption and desorption, CO insertion, H_2 dissociation, and hydrogenation, *etc*., and the effects of them change with the doping content.

The results indicated that the doping of Mn can change the Rh valence and dispersion. With regards to the CO adsorption, these changes can enhance the CO adsorption ability of Rh and weaken the CO-Rh bond strength very effectively when the amount of Mn reached 1.5 wt.%. Improved capacity of CO adsorption is conducive to increase of CO conversion, while the weakening of CO-Rh bond is beneficial to CO insertion reaction, thus contributing to the generation of C_2^+ oxygenates. Moreover, the low amount of Li ($\leq$0.075 wt.%) can also enhance the CO adsorption, resulting in the improvement of reactivity. But an opposite effect appeared at high content of Li (>0.075 wt.%).

On the other hand, Mn and Li promoted dissociation of H_2, which is favorable to increase the rate of hydrogenation. However, when the content of Mn exceeded 1.5 wt.%, the promotion effect would be weakened.

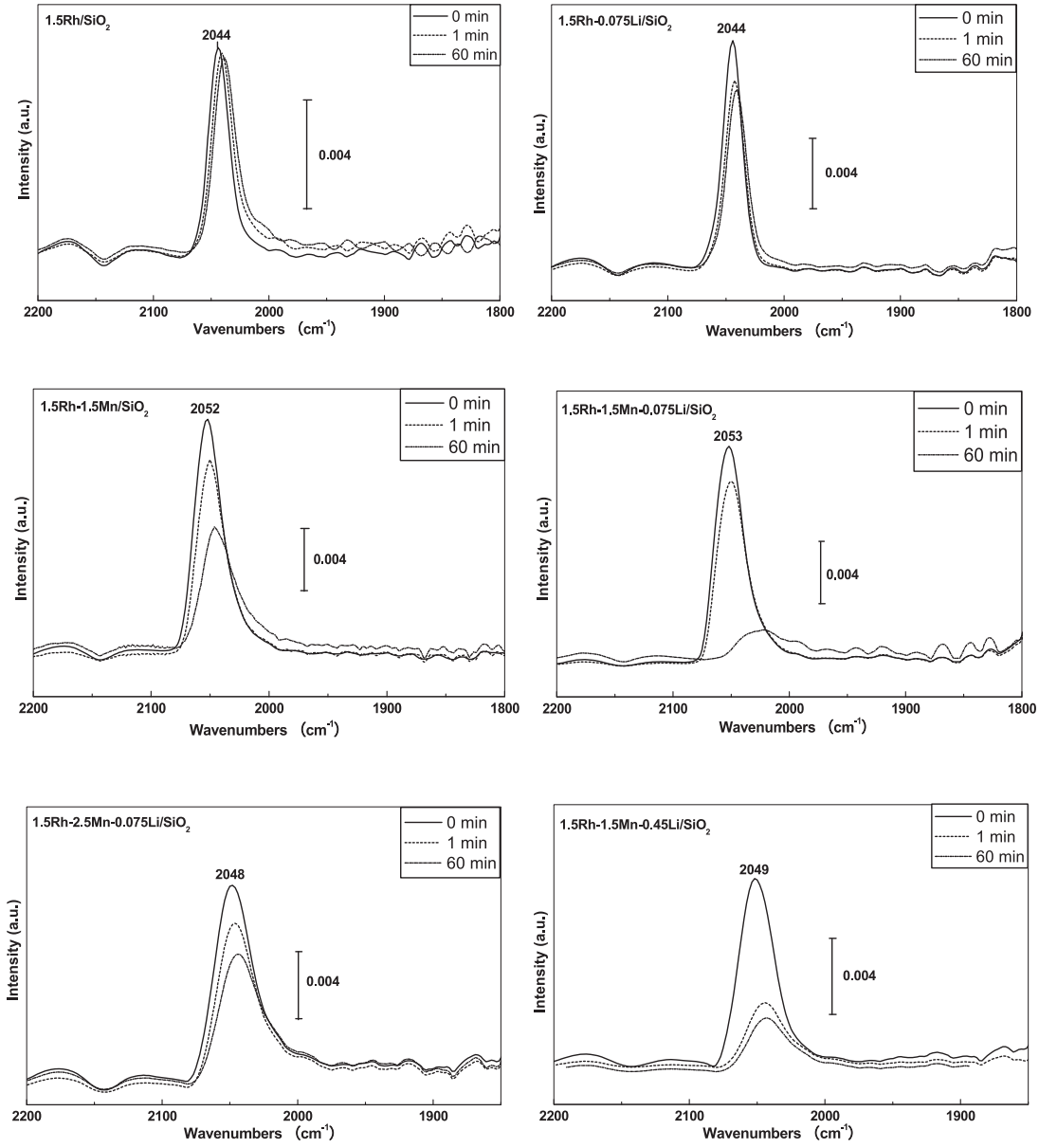

Fig. 7. The infrared spectra after CO hydrogenation on different catalysts at 300 °C.

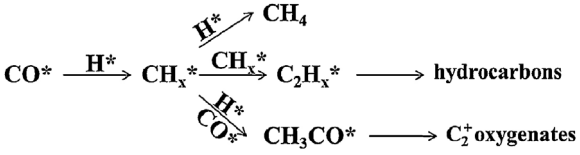

Fig. 8. Mechanism for synthesis of C_2^+ oxygenates from syngas.

Generally, the mechanism for synthesis of C_2^+ oxygenates from syngas is proposed (see Fig. 8) as follows [29,30]. The adsorbed CO dissociation and hydrogenation to produce CH_x species is likely the first step, although it remains unclear whether C—O bond cleavage occurs through direct breaking of this bond in an adsorbed CO or by a process involving hydrogen. The CH_x species then undergoes: (a) formation of C_2^+ oxygenates precursor of CH_xCO by CO insertion, or (b) hydrogenation to form methane, or (c) chain growth to form higher hydrocarbons. According to this mechanism, the increase of CO adsorption capacity is an important contributor to CO conversion. Meanwhile, if the hydrogenation capacity is weak, the catalytic activity should also be restrained. It is usually considered that the formation of hydrocarbons from CH_x hydrogenation and the formation of C_2^+ oxygenates from CO insertion are the couple of competitive reaction, and the relative reaction rate between them determines the activity and selectivity forwards C_2^+ oxygenates. Thus, considering that the weakening of Rh-CO band strength is conducive to the reaction of CO insertion, which should be responsible for the higher C_2^+ oxygenates selectivity. As the optimized results, when Rh, Mn, Li content was 1.5 wt.%, 1.5 wt% and 0.075 wt%, the catalyst for CO hydrogenation of C_2^+ oxygenates achieved the best performance.

4. Conclusion

The roles of the loading of Mn and Li promoters in the catalytic performance for the synthesis of C_2^+ oxygenates from syngas on Rh-Mn-Li/SiO_2 catalysts were explored. The results showed that, the synergy of Rh-Mn-Li can increase the CO conversion and C_2^+ oxygenates selectivity. As the increase of Mn loading, the

C_2^+ oxygenates decreased ceaselessly; while the CO conversion had the maximum when the Mn content reached 1.5 wt.% and decreased rapidly when the amount of Mn exceeded 1.5 wt.%. The addition of Li could both improve the CO conversion and C_2^+ oxygenates selectivity when the doping amount was very low (0.075 wt.%); and high amount of Li addition (0.45 wt.%) would reverse this effect.

Our results seem to suggest that the changes in catalytic performances observed here are due to changes in the catalyst abilities of CO adsorption, CO insertion, H_2 dissociation, and hydrogenation, *etc*., which are mainly controlled by the states of Rh.

The XPS analysis showed that Rh existed mainly as metallic Rh after reduction. Due to the interaction of Rh-Mn, some partially positively charged $Rh^{\delta+}$ species appeared on the surfaces of the reduced catalysts containing Mn promoter. The results of H_2-TPR indicated the intensity of Rh-Mn interaction is related to the Mn/Rh ratios. Increasing the ratio of Mn/Rh, the most effective interaction of Rh-Mn was reached when the ratio of Mn/Rh = 1.

The results of IR showed that, with a reasonable rate of Rh/Mn, the addition of Mn can enhance the CO adsorption ability of Rh and weaken the CO-Rh bond strength very effectively. And the low doping of Li can not only enhance the CO adsorption capacity, but also improve the dissociation of H_2. The increase of CO adsorption capacity can help to improve the rate of CO conversion, and the weakened CO-Rh bond strength is beneficial for the CO insertion reaction, which promoted the generation of C_2^+ oxygenates. On the other hand, the promotion of H_2 dissociation is favorable to increase the rate of hydrogenation. As the optimized results, when Rh, Mn, Li content was 1.5 wt.%, 1.5 wt.% and 0.075 wt.%, the catalyst for CO hydrogenation of C_2^+ oxygenates achieved the best performance.

Acknowledgments

The authors gratefully acknowledge financial support from the Science and Technology Commission of Shanghai Municipality (08520513600), Leading Academic Discipline Project of Shanghai Education Committee (J51503) and Shanghai Municipal Science and Technology Commission (13ZR1461900).

References

[1] J.J. Spivey, A. Egbebi, Chem. Soc. Rev. 36 (2007) 1514–1528.
[2] J.R. Rostrup-Nielsen, Science 308 (2005) 1421–1422.
[3] D.H. Mei, R. Rousseau, S.M. Kathmann, V.A. Glezakou, M.H. Engelhard, W.L. Jiang, C.M. Wang, M.A. Gerber, J.F. White, D.J. Stevens, J. Catal. 271 (2010) 325–342.
[4] A.E. Farrell, R.J. Plevin, B.T. Turner, A.D. Jones, M. O'Hare, D.M. Kammen, Science 311 (2006) 506.
[5] R.P. Underwood, A.T. Bell, Appl. Catal. 21 (1986) 157–168.
[6] H. Ehwald, H. Ewald, D. Gutschick, M. Hermann, H. Miessner, G. öhlmann, E. Schierhorn, Appl. Catal. 76 (1991) 153–169.
[7] M. Ojeda, M.L. Granados, S. Rojas, P. Terreros, F.J. García-García, J.L.G. Fierro, Appl. Catal. A: Gen. 261 (2004) 47–55.
[8] X.L. Pan, Z.L. Fan, W. Chen, Y.J. Ding, H.Y. Luo, X.H. Bao, Nat. Mater. 6 (2007) 507–511.
[9] J. Gao, X. Mo, A.C. Chien, W. Torres, J.G. Goodwin Jr., J. Catal. 262 (2009) 119–126.
[10] S.S.C. Chuang, G. Srinivas, M.A. Brundage, Energy Fuels 10 (1996) 524–530.
[11] R. Burchand, M.J. Hayes, J. Catal. 165 (1997) 249–261.
[12] B.J. Kip, P.A.T. Smeets, J.H.M.C. Van Wolput, H.W. Zandbergen, J. Van Grondelle, R. Prins, Appl. Catal. 33 (1987) 157–180.
[13] P.Z. Lin, D.B. Liang, H.Y. Luo, C.H. Xu, H.W. Zhou, S.Y. Huang, L.W. Lin, Appl. Catal. A 131 (1995) 207–214.
[14] W.M.H. Sachtler, M. Ichikawa, J. Phys. Chem. 90 (1986) 4752–4758.
[15] Y. Wang, H.Y. Luo, D.B. Liang, X.H. Bao, J. Catal. 196 (2000) 46–55.
[16] R. Ugo, Catal. Rev. 11 (1975) 225–297.
[17] S.C. Chuang, J.G. Goodwin, I. Wender, J. Catal. 95 (1985) 435–446.
[18] J. Yu, D.S. Mao, G.Z. Lu, Q.S. Guo, L.P. Han, Catal. Commun. 24 (2012) 25–29.
[19] J. Yu, D.S. Mao, L.P. Han, Q.S. Guo, G.Z. Lu, J. Mol. Catal. A: Chem. 367 (2013) 38–45.
[20] M. Szekeres, O. Kamalin, P.G. Grobet, R.A. Schoonheydt, K. Wostyn, K. Clays, A. Persoons, I. Dkénáy, Colloids Surf. A: Physicochem. Eng. Aspects 227 (2003) 77–83.
[21] J. Raskó, J. Bontovics, Catal. Lett. 58 (1999) 27–32.
[22] H.M. Yin, Y.J. Ding, H.Y. Luo, H.J. Zhu, D.P. He, J.M. Xiong, L.W. Lin, Appl. Catal. A: Gen. 243 (2003) 155–164.
[23] D.H. Jiang, Y.J. Ding, Z.D. Pan, X.M. Li, G.P. Jiao, J.W. Li, W.M. Chen, H.Y. Luo, Appl. Catal. A: Gen. 331 (2007) 70–77.
[24] W.M. Chen, Y.J. Ding, D.H. Jiang, G.P. Jiao, H.J. Zhu, Z.D. Pan, H.Y. Luo, Chin. J. Catal. 27 (2006) 999–1004.
[25] S.D. Worley, G.A. Mattson, R. Caudlll, J. Phys. Chem. 87 (1983) 1671–1673.
[26] R.R. Cavanagh, J.T. Yates Jr., J. Chem. Phys. 74 (1981) 4150–4155.
[27] C.A. Rice, S.D. Worley, C.W. Curtis, J.A. Guin, A.R. Tarrer, J. Chem. Phys. 74 (1981) 6487–6497.
[28] F. Solymosi, M. Pasztor, J. Phys. Chem. 89 (1985) 4789–4793.
[29] M. Ichikawa, Chem. Tech. 12 (1982) 674–680.
[30] Y. Choi, P. Liu, J. Am. Chem. Soc. 131 (2009) 13054–13061.
[31] P. Winslow, A.T. Bell, J. Catal. 86 (1984) 158–172.